ANALYSIS OF A FAST-SPREADING RISE CREST: THE EAST PACIFIC RISE, 9° TO 12° SOUTH

DAVID K. REA*

School of Oceanography, Oregon State University, Corvallis, Oregon 97331, U.S.A.

(Received 1 March, 1976; revised 17 May, 1976)

Abstract. The axis of the East Pacific Rise is defined by a topographic block about 15 km wide and 300 to 350 m high which is flanked by abyssal hills 100 to 200 m high and 3 to 5 km wide. These hills often are tilted such that their steep slopes face the axis. An empirical model explaining these features combines axial extrusion to form the central block and rotational faulting to lower the shoulders of the axial block to the regional depth and tilt them outward.

The axial block is offset about 10 km left-laterally at 10.0°S and a similar amount right-laterally at 11.5°S. Offsets (or lack of offsets) of young magnetic anomalies indicate that these axial displacements occurred between 1.7 and 0.9 m.y. ago and 0.7 m.y. ago and the present in the north and south, respectively. These small axial offsets are interpreted to be the result of either brief episodes of asymmetric sea-floor spreading or discrete jumps in the site of spreading activity. Both axial shifts were to the west; a unidirectional sequence of such shifts occurring at the above rate of one per million years would be difficult to differentiate from true regional asymmetric spreading and might explain that phenomenon on other medium-to fast-spreading rises.

Reconnaissance data from the east flank of the East Pacific Rise indicate that spreading activity began on that part of the rise between the 9°S and 13.5°S fracture zones approximately 8.2 m.y. ago when the site of crustal accretion jumped westward from the now dormant Galapagos Rise. Slope change in crust approximately 2 and 6 m.y. old imply faster spreading rates between about 6 and 2 m.y. ago than either before or after that time. Identification and correlation of anomaly 3′ allows an estimate of about 90 mm/y for this higher east flank spreading rate. Since 1.7 m.y. ago spreading rates have averaged about 80 mm/y to the west and 77 mm/y to the east.

1. Introduction and Data

The western margin of the Nazca lithospheric plate is formed by that portion of the East Pacific Rise (EPR) lying between the Galapagos triple junction at 2°N and the Easter Island triple junction at 34°S (Figure 1). Geologically, the modern EPR is a young feature, which is thought to have come into existence between about 25 and less than 10 million years (m.y.) ago as spreading activity in the eastern Pacific shifted several hundred kilometers westward from the now fossilized Galapagos Rise (Herron, 1972). The portion of the EPR between the two triple junctions has the most rapid sea-floor spreading rates found along the entire world rift system, with half-rates ranging from about 80 mm/y in the northern portion (Rea *et al.*, 1973), to 100 mm/y further south (Herron, 1972).

This paper presents the results of a detailed survey of the EPR crest at about 10.5°S and of several reconnaissance lines that traverse the east flank of the rise. Five cruises were made to the EPR between 9° and 12°S between late 1971 and 1973

* Present address: Department of Atmospheric and Oceanic Science, University of Michigan, Ann Arbor, Michigan 48105, U.S.A.

Marine Geophysical Researches **2** (1976) 291–313.

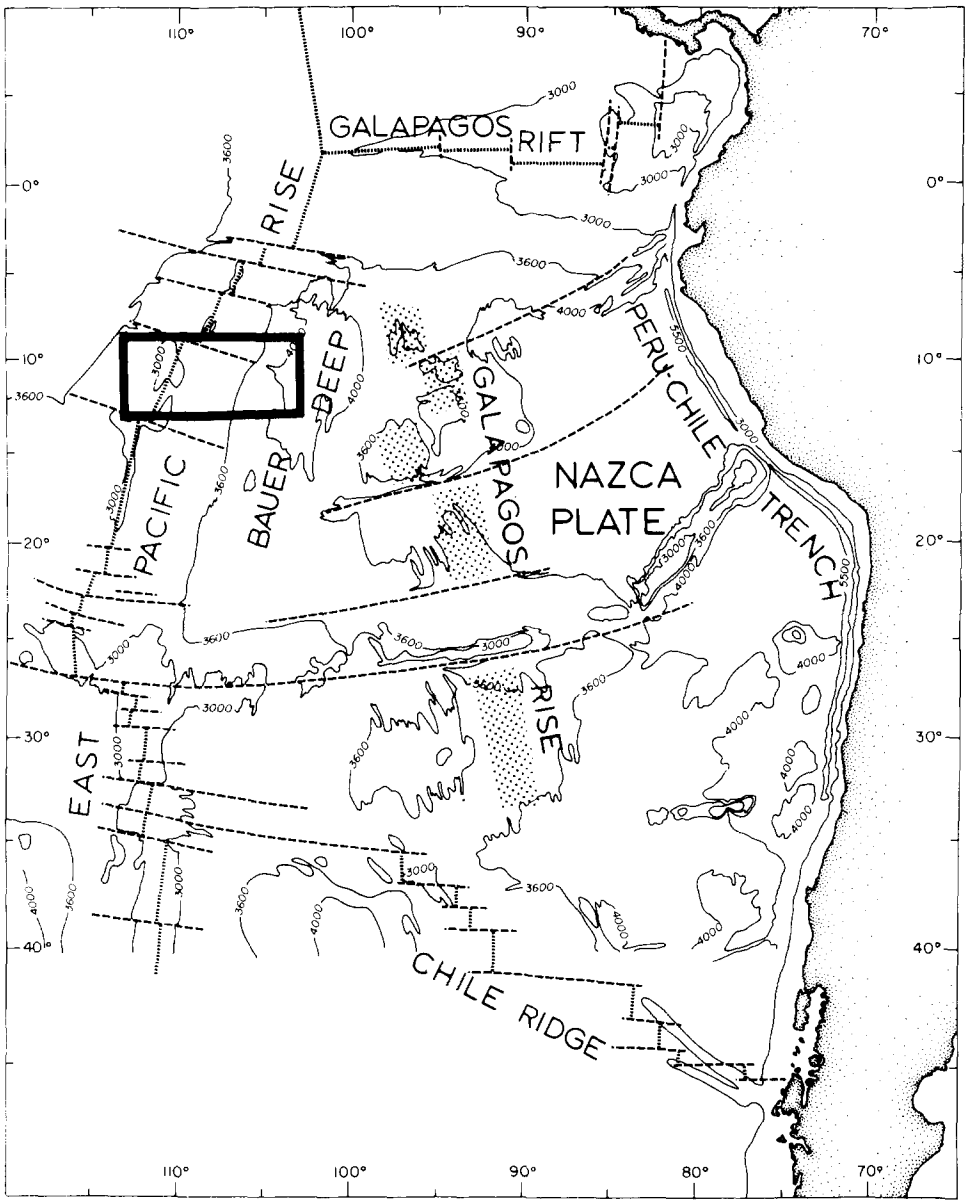

Fig. 1. Index map of the Nazca Plate. Study area is outlined by heavy black line. Locations of the East Pacific Rise, Bauer Deep, and extinct Galapagos Rise (light stipple) are shown.

under the auspices of the IDOE Nazca Plate Project (Figure 2). These cruises include two by the R/V *Kana Keoki* of the Hawaii Institute of Geophysics, KK-71-7 traverse along 12°S, and KK-71-8 to the EPR survey area at 10.5°S; one by the R/V *Yaquina* of Oregon State University, YALOC-71-7 to the 10.5°S survey area; and two cruises of the NOAA Ship Oceanographer, Oceo-73-1 and Oceo-73-4. Data

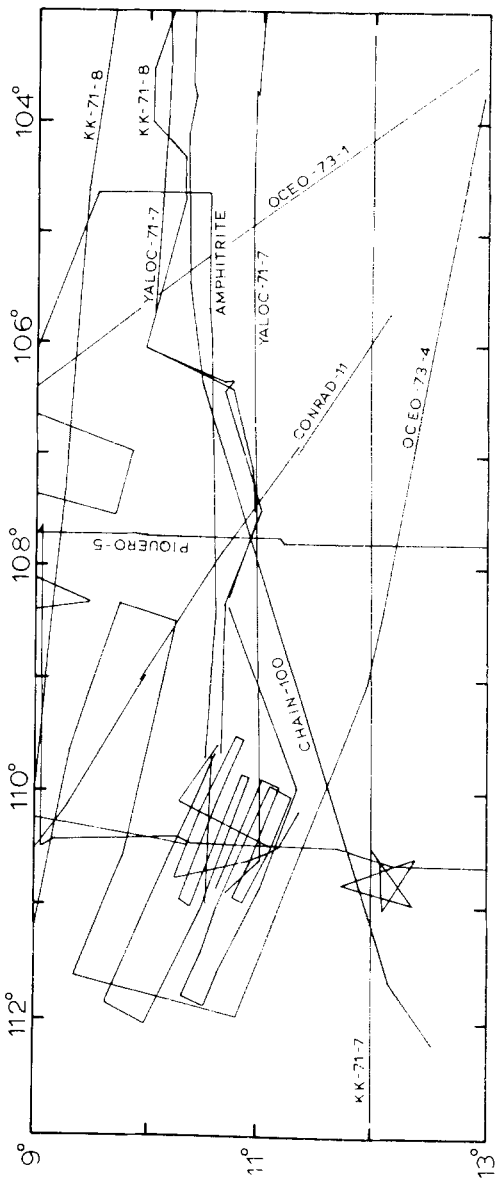

Fig. 2. Tracklines within the study area.

from previous cruises were kindly supplied by the other institutions (see Acknowledgements; Figure 2).

All cruise tracks since about 1968 or 1969 are located by satellite navigation with an accuracy of location of better than 1 km and generally better than 0.5 km. The detailed survey area at 10.5°S was completed entirely with satellite navigation and the agreement of data at line crossings is excellent.

During all of the Nazca Plate Project cruises, routine underway data gathering operations included bathymetric observations, either by 12 kHz or 3.5 kHz echo sounders, magnetic observations with a proton-precession magnetometer, and gravity observations using Lacoste–Romberg stable-table meters. For most of the cruises, low-frequency seismic-reflection data were also collected. All bathymetric data used in constructing the contour map of the survey area were corrected for the variation of sound velocity in seawater utilizing the Matthews Tables (Matthews, 1939). Total intensity magnetic data were reduced to anomaly form using the International Geomagnetic Reference Field (IAGA Commission 2 Working Group 4, 1969).

The data presented here bear upon several problems concerning the tectonic regime of the East Pacific Rise and fast-spreading rises in general. The location of the 10.5 °S survey area was chosen because existing reconnaissance data indicated that the region was geologically simple and therefore a good place to study the normal development of the rise axis. Results of such a study are basic to our knowledge of fast-spreading rises and prerequisite to examination of the more complicated sections of the EPR axis.

The westward jump of the southeast Pacific spreading center is moderately well documented (Herron, 1972; Anderson and Sclater, 1972; Mammerickx *et al.*, 1975), but the exact timing of this shift, which occurred in segments, is not yet known. Several reconnaissance lines traversing the east flank of the EPR between 9° and 13°S permit reconstruction of the tectonic history of this region, including a more accurate estimate of the time of inception of spreading activity.

Axis jumps on the order of tens of kilometers also may occur along the EPR. Data presented below define two such small offsets and their time of occurrence, but are not sufficient to distinguish between the two possible mechanisms that could result in these small offsets.

2. East Pacific Rise Axial Region

2.1. The 10.5 ° Survey area

A. *Bathymetry*

In February 1972, the R/V *Yaquina* of Oregon State University and R/V *Kana Keoki* of the Hawaii Institute of Geophysics surveyed in detail a portion of the EPR crest centered at about 10.5°S. A bathymetric contour map of the 10.5°S survey area (Figure 3) depicts the typical features of the EPR crest. The precise axis of the EPR is

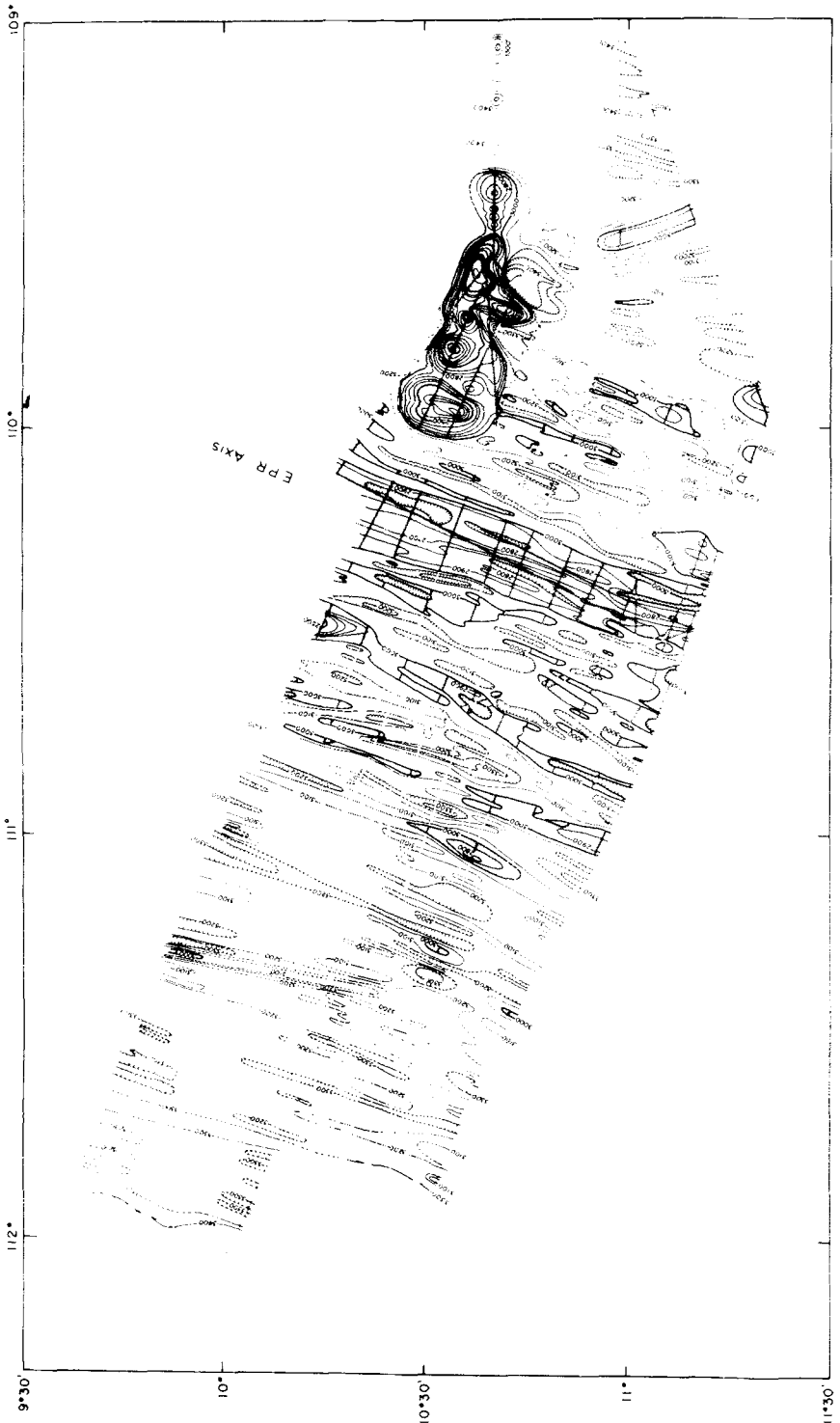

Fig. 3. Bathymetric map of the 10.5°S survey area. Depths are in corrected meters; contour interval is 100 m. Regions less than 3000 m deep are shaded.

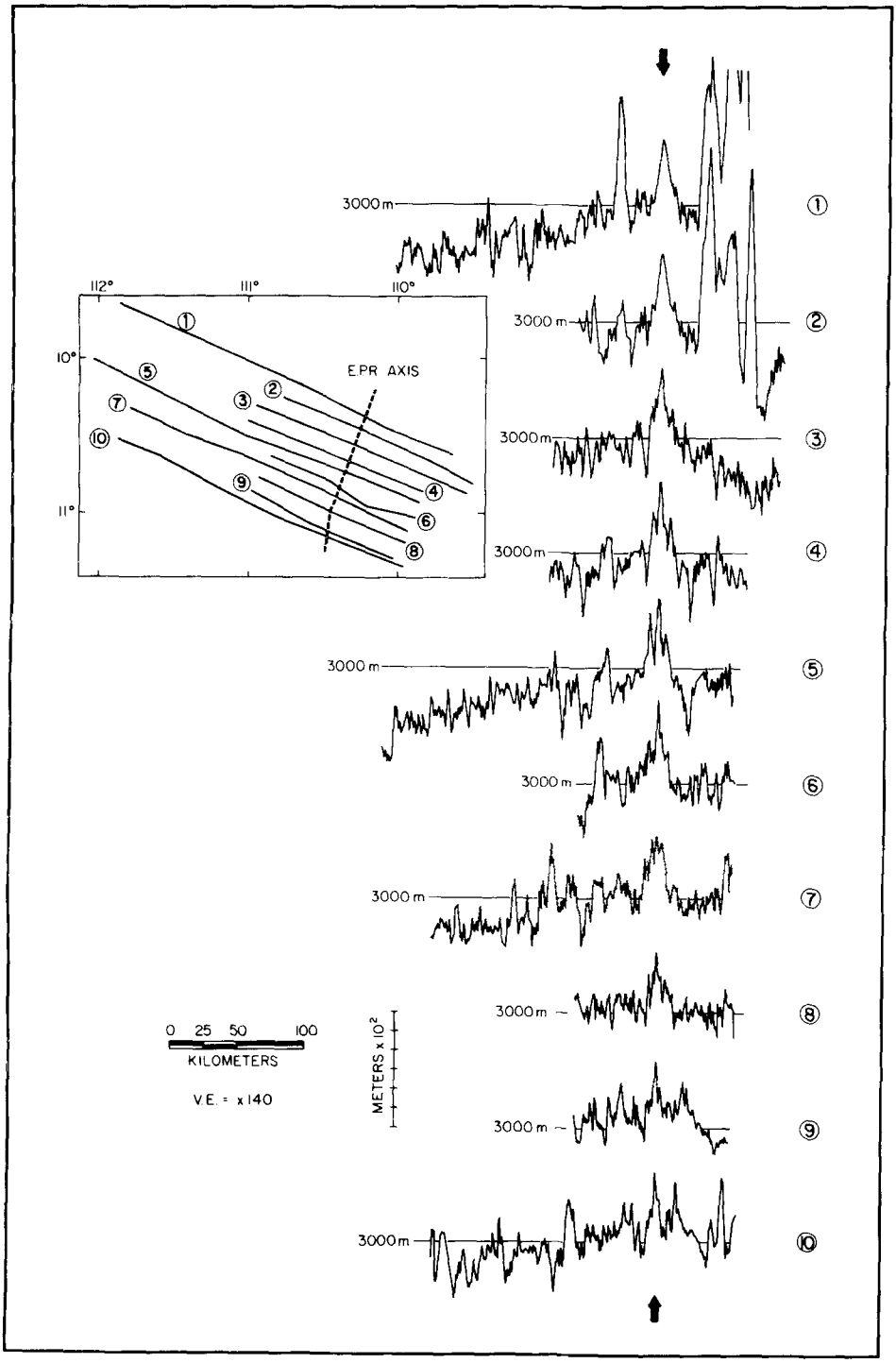

Fig. 4. Bathymetric profiles from the 10.5° S survey area. Trackline locations given by inset. West is to the left. Profiles are aligned on the EPR axial block (arrows).

a topographic block about 300 m high and 15-20 km wide (Figures 3 and 4). The shallowest depth of this block is usually about 2700 m and the 3000 m contour line (Figure 3) generally defines its lateral extent. The axis displays a remarkable linearity along a trend of 018° in the northern two-thirds of the area, but changes trend at 11°S to 012° in the southern portion of the survey area. This trend change is confirmed by reconnaissance tracklines to the south of the survey area. Shoulders commonly occur along the axial block, and where well developed (Figure 4, lines 4 and 5), divide the axial block into three peaks of sub-equal width; the middle peak in all cases is the highest one. Such an axial block characterizes the East Pacific Rise throughout much of its length (Anderson and Noltimier, 1973).

Away from the axial block, the topography of the upper flank of the EPR is characterised by abyssal hills of 100 to 200 m relief. These hills and the intervening valleys are lineated parallel to the rise axis and some of them may be continuous across the entire area surveyed. More commonly these features are 20 to 30 km long. Bathymetric profiles (Figure 5) show that this abyssal topography has a wavelength of 3 to 5 km and also that the small hills seem to group into units, or blocks, that are 20 to 30 km wide (Figures 4 and 6). A large seamount occurs in the northeast portion of the survey area (Figure 3). The seamount is elongated perpendicular to the EPR axis and has horizontal dimensions of approximately 60 by 20 km. Its relief is about 1500 m with a least depth of approximately 1750 m.

Sediment cover in the survey areas is so thin and patchy that the seismic-reflection profiles show only bathymetry. With only bathymetric data it is not easy to differentiate between tectonic (faulting) and volcanic (extrusion paralleling the axis) origins for the abyssal hills. Data from deeply-towed instruments have provided evidence for the faulting origin of abyssal hills found near other spreading centers by demonstrating that many of the slopes on the 3 to 5 km wavelength topography are fault scarps of various dimensions (Luyendyk, 1970; Larson, 1971; Atwater and Mudie, 1973; Klitgord and Mudie, 1974). Thus, it seems profitable to analyze the topography for probable fault-bounded features. Bathymetric profiles from the 10.5 °S survey area appear to contain two different wavelengths of topography. The higher frequency topography is three to five kilometers in wavelength (Figure 5) and is superimposed upon blocks whose wavelengths measure a few tens of kilometers (Figure 4). In an attempt to validate this intuitive conclusion, a spectral analysis was performed on the topography of the four longer survey lines (Figure 4, lines 1, 5, 7 and 10). Results of the spectral analysis give the distribution of the variance of the topography with respect to frequency. By this method it can be shown, depending on the line analyzed, that 95 percent of the variance, or divergence from a linear slope, lies in topography having wavelengths greater than 3.5 to 5 km. Thus, although these smaller features are the predominant wavelength, they are essentially randomly distributed noise superimposed on a signal of longer wavelength.

The second step in this procedure is to remove the higher frequency noise and ascertain what sort of signal remains. To do this we first interpolated the data to a constant sample interval of 1 km and then took an N-point moving average of the

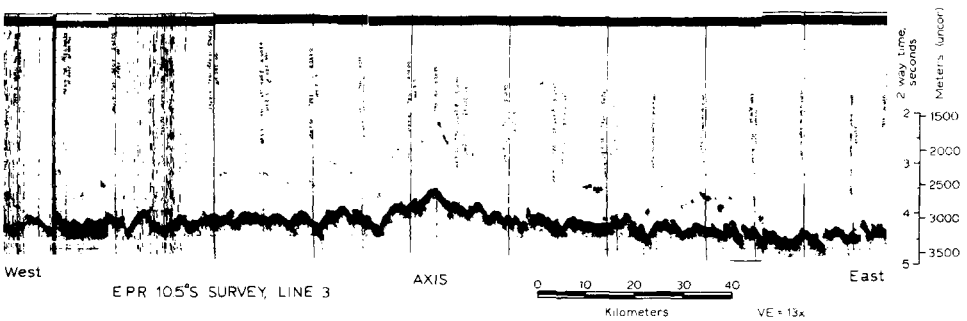

Fig. 5. Original bathymetric record of line 3 of the 10.5°S survey area. Profile location is shown on Figure 4.

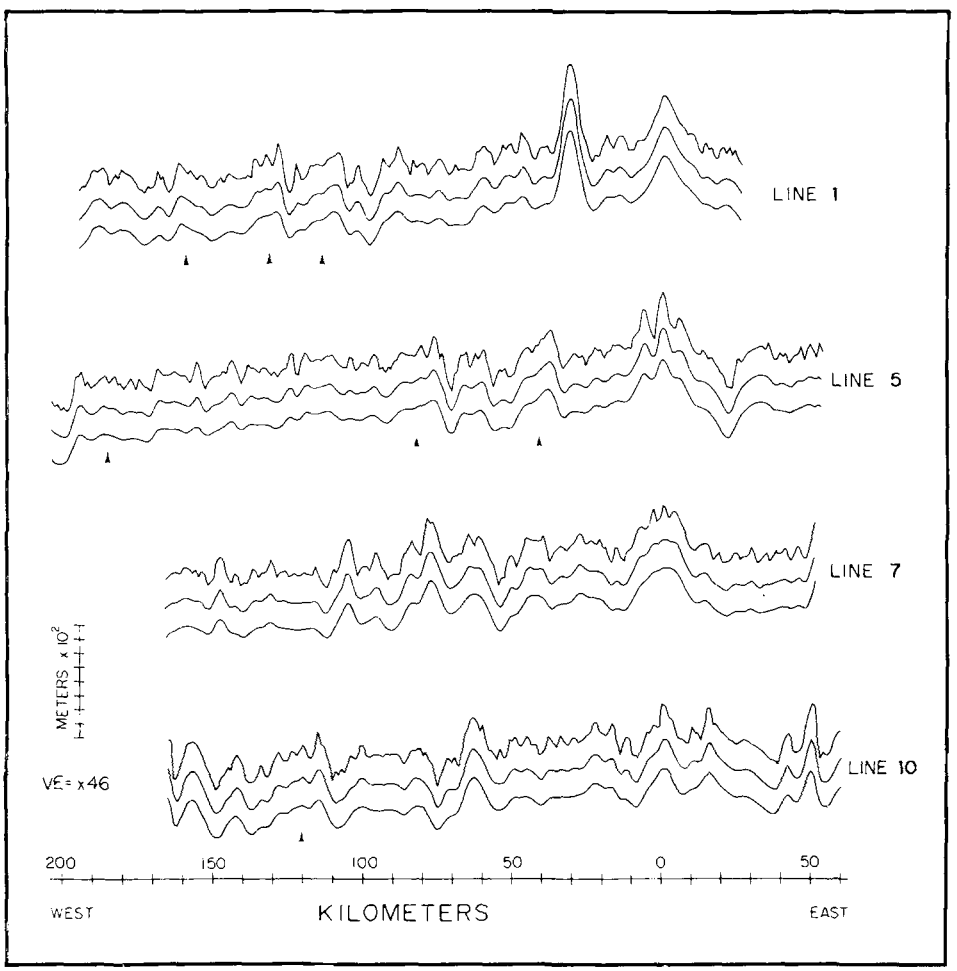

Fig. 6. Filtered bathymetric profiles, 10.5°S survey area. Top line is original data interpolated to 1 km data spacing. Middle and bottom lines are 5- and 9-point weighted moving averages, respectively, of top line. Tilted blocks are indicated by arrows. Kilometer scale is zero at EPR axis. Profile locations are on Figure 4.

data, weighted with a Gaussian distribution. This method weights the data near the center of the window more heavily than those near the edges, thereby limiting the effect of local bathymetric extremes. Five points considered together span a 4 km interval and attentuate the 3 to 5 km wavelength topography.

Results of this procedure, using both a 5- and 9-point moving weighted average, are illustrated in Figure 6. When the shorter wavelengths are filtered out longer wavelengths become more apparent. Filtered profiles (Figure 6) reveal a series of topographic blocks, 10 to 30 km wide. Most of these blocks are either tilted away from the EPR axis or untilted. A few, especially at the extreme western ends of lines 1 and 5 (Figure 6), are tilted toward the axis.

It is likely that these blocks, 10–30 km wide and, from Figure 3, perhaps 30–50 km long, are the result of normal faulting of the ocean floor. When faults dip toward the axis, the tops of the blocks are rotated away from the axis. More rarely, when faults dip away from the axis the block tops are rotated toward the axis. This faulting will be discussed in more detail below.

Thus, there appears to be at least three scales of faulting of the EPR, forming three sizes of features. Small faults spaced a few hundred meters apart produce small asymmetrical hills a few tens of meters high (Larson, 1971). Faults spaced a few kilometers apart produce asymmetrical hills with about 100 m relief (Klitgord and Mudie, 1974). This scale of faulting probably produces the 3–5 km topography seen in Figures 3–5. And finally, faults spaced several tens of kilometers apart may result in tilted blocks of that width and perhaps 200 m in total relief.

B. *Magnetic Anomalies*

At 10.5 °S, the crest of the East Pacific Rise is within a few degrees of the equator and lies in a zone where anomalies are often difficult to interpret. The trend of the EPR axis is not far from north, a geometric condition that results in low amplitude sea-floor spreading magnetic anomalies. Conversely, any cross structures, such as abyssal hill terminations or small fracture zones, would produce much higher amplitude anomalies (Schouten, 1971; Rea, 1972).

A map of the magnetic anomalies in the 10.5°S survey area illustrates their general irregularity (Figure 7). In contrast to magnetic anomaly maps of most other ridge-crest regions, there are no obvious sea-floor spreading anomaly stripes extending across this area. The only feature on the map approaching such a stripe is the north-northeast trending anomaly near 111°W.

The most obvious magnetic features on the map are in the northeastern portion of the survey area and are related to the large seamount. These anomalies vary from less than -700γ to more than $+200\gamma$. The largest anomaly coincides with the shallowest peak of the seamount. The irregular nature of the anomalies associated with this seamount is somewhat surprising as many similar sized and larger seamounts and/or volcanic ridges have been mapped elsewhere (cf. Rea and Naugler, 1971) and almost all of them have reasonably regular dipole anomalies associated with them. Simple magnetic models of this feature suggest that the irregular magnetic

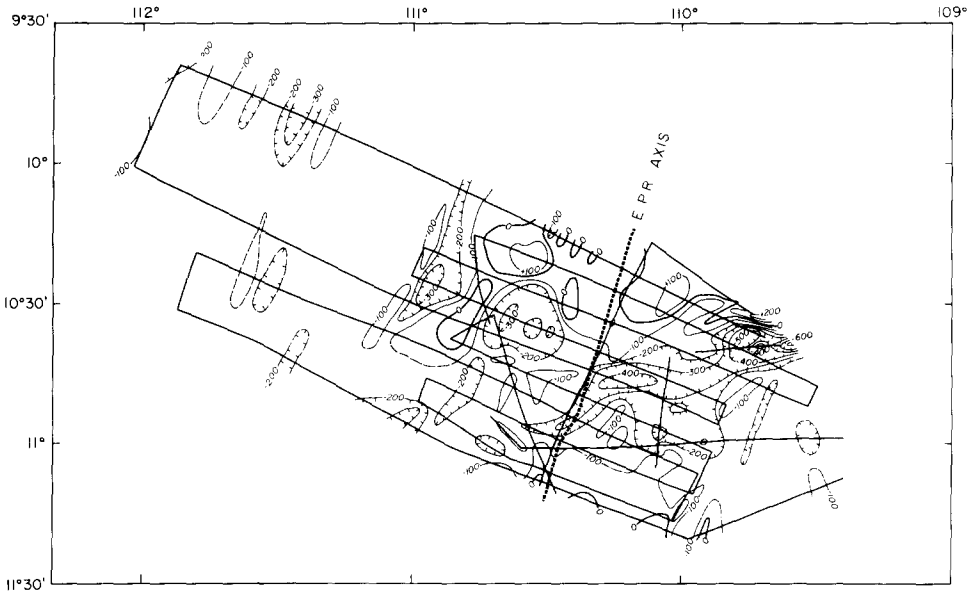

Fig. 7. Magnetic anomaly map of the 10.5°S survey area. Contour interval is 100 gammas.

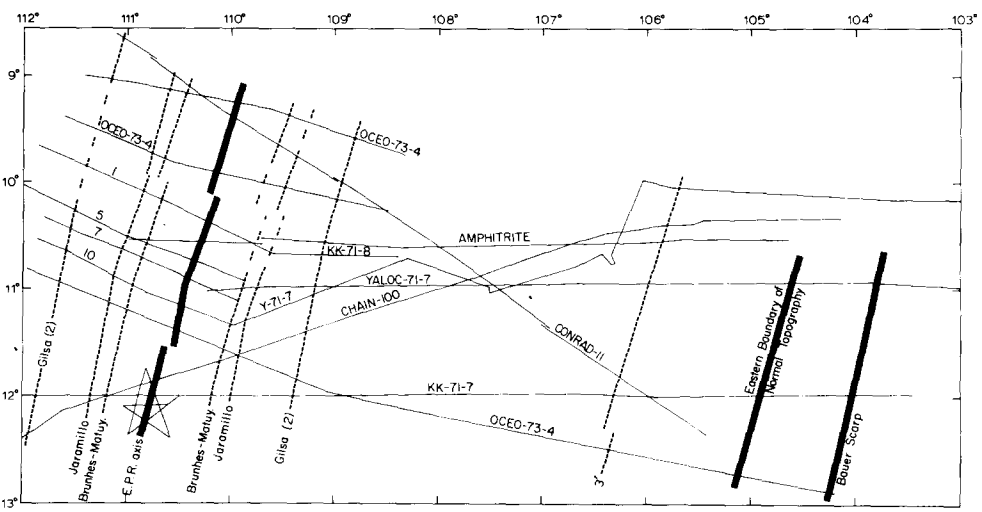

Fig. 8. Map of the EPR showing magnetic anomaly (dashed lines) and bathymetric (heavy lines) correlations.

anomalies associated with it result from structural complexities within the seamount.

A linear, negative magnetic anomaly crosses the EPR axis at about 11.0°S, 110.4°W, turns northeast parallel to the axis, then east to merge with the seamount anomalies at 109.8°W (Figure 7). At the point where the anomaly intersects the axis, the axis changes trend from 018 ° to the north to 012° to the south (Figures 3 and 8).

The negative anomaly implies normal polarization of any material intruded into a fracture and the most intense portion (outlined by the -400γ contour, Figure 7) may represent either the widest portion of the intrusion or the part trending most nearly east-west.

Away from the axis this east-west trending anomaly does not correspond to any comparable structure or trend in the bathymetry (Figure 3). Continuation of this east-west trending magnetic anomaly into those produced by the seamount implies a structural relation between the two, as if an oblique fault were intruded but the intrusion breached the surface at only one place and did not disturb or influence the local abyssal topography elsewhere.

Two broad oval-shaped anomalies, 25 to 35 km in diameter, occur west of the EPR axis (Figure 7). The northern anomaly is positive and the southern one is negative. The origin of these features is unknown, although certainly the southern one and probably the northern one are real and not the result of aberrations along only one trackline. Application of half-width methods (Dobrin, 1960) imply a maximum depth to source of 20 to 30 km for these features. At this depth, the material should be well within the magma chamber underlying the EPR (Scheidegger, 1973) and the temperature far above the Curie point. Hence, the origin of these broad magnetic features remains unclear, although their source must be broad and shallow.

2.2. Geology of the axial region

The axial region of the East Pacific Rise between the 9°S fracture zone and 12°S can be divided into three sub-regions by two small axial offsets occurring at 10.0°S and 11.5°S (Figure 8). Linear magnetic anomalies mapped on Figure 8 are taken from magnetic profiles (Figure 9) where they are more readily observed rather than from the magnetic anomaly map (Figure 7) where they are not obvious. In the northern two sub-regions the axis position is approximately centered within the magnetic anomalies on either flank. The central sub-portion is offset about 8 to 10 km from the northern portion at approximately 10.0°S, implying the existence of either a sharp double bend in the ridge axis or a small transform fault with left lateral offset. This small offset evidently has existed for at least 0.9 m.y. as both the Jaramillo and Brunhes/Matuyama anomalies are symmetrical about the axis segments and are offset by similar amounts as the axis. The Gilsa anomaly (nomenclature of Cox, 1969) to the east apparently is unaffected by this offset, implying that the offset originated sometime between about 1.6 and 1.0 m.y. ago. Definition of the Gilsa anomaly west of the small offset, however, is ambiguous.

Within the central sub-portion of this region, defined mostly by the detailed survey, the EPR axial block changes trend from 018° to 012° south of 11°S. As is the case for the offset at 10.0°S, the Jaramillo and Brunhes/Matuyama anomalies reflect this change in trend but the Gilsa anomaly shows little or no change. This indicates that the change in trend may have occurred some time between 1.6 and 1.0 m.y. ago.

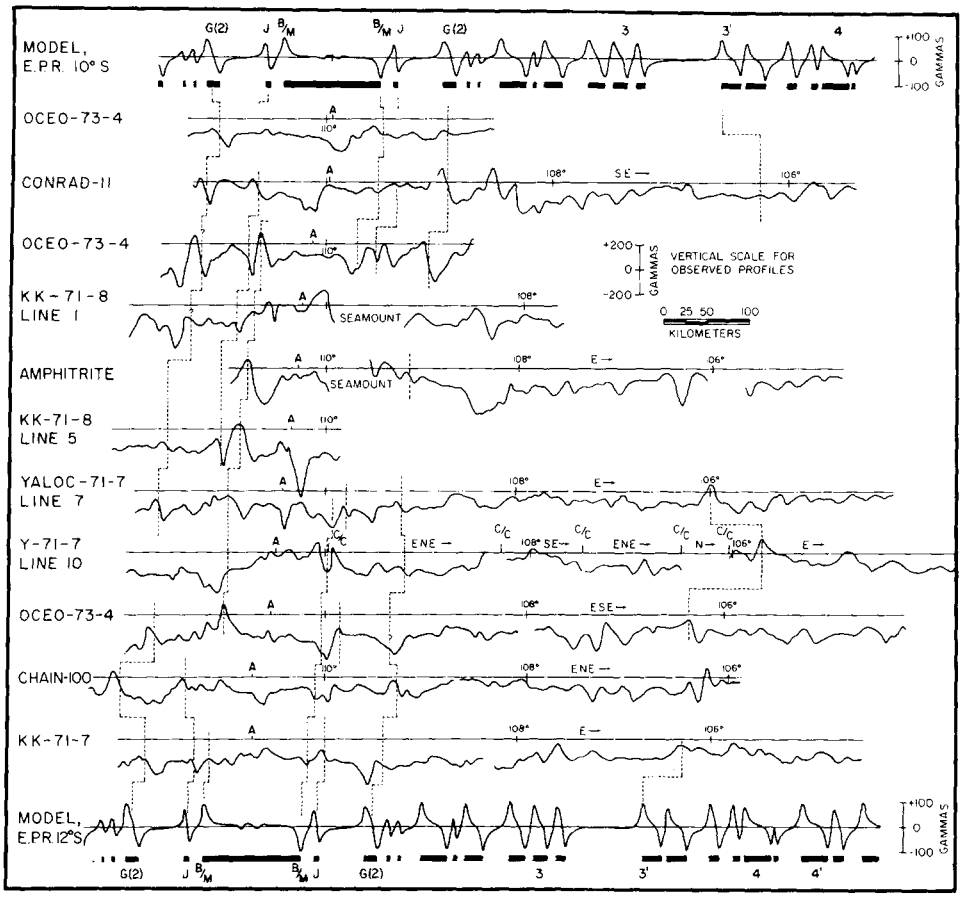

Fig. 9. Magnetic anomaly profiles with correlations, EPR 9° to 12°S. Model parameters include the general time scale of Cox (1969), 80 mm/y spreading rate, 3.5 to 4.0 km magnetized layer with remanent magnetization of 0.025 emu/cc, and a profile trend of 108°. B/M is the Brunhes/Matuyama boundary, J and G the Jaramillo and Gilsa events. Anomaly numbers are according to Heirtzler and others (1968). Profile locations are on Figure 8. A denotes EPR axis, determined topographically. Profiles trend southeasterly except where noted. West is to the left.

Along 12°S, the small star-survey run by the *Kana Keoki* and the *Chain*-100 trackline (Figure 8) define the EPR axial block in the southern portion of the region. Northward extension of the axis as mapped at 12°S does not meet the axis as defined in the southern portion of the 10.5°S survey area. Another double bend or small transform fault must therefore occur at about 11.5°S. This offset is right lateral in sense. Unlike the small offset at 10.0°S, the axial offset in the southern portion of the region is not reflected in the magnetic anomalies and at 12°S the EPR axis lies 10 km west of a median line between the flanking Brunhes/Matuyama anomalies (Figure 8). This means that this offset formed sometime during the last 0.69 m.y., between the time of the Brunhes/Matuyama reversal and the present. Both offsets, therefore, originated within a maximum time span of about 0.6 m.y.

These ridge offsets could be produced by either of two mechanisms. One of these entails a rather brief episode of highly asymmetric sea-floor spreading along a portion of the rise axis. In the case of the axial asymmetry at 12°S (Figure 8) the east flank spreading rate must have been approximately 50 percent faster than the west flank rate during the last 0.69 m.y. As well as being temporally restricted, the area affected by asymmetric spreading would have to have fairly sharp lateral boundaries along the rise axis.

Alternatively, the axis shift could be accomplished by a small jump in the location of the spreading center. Such a jump could occur if one of the faults bounding the axial block (see below) propagated deep enough to tap the underlying magma chamber and then became the preferred axis of extrusion. Such an event would shift the spreading center a distance roughly equal to the half-width of the axial block, 8 or 10 km, an amount equal to the observed offsets in the EPR axis.

Available data do not indicate which of these two explanations, true asymmetrical spreading or discrete axial jumps, is the correct one. The data do suggest, however, that an active ridge axis can change its location and trend, within some prescribed limits, over relatively short periods of time. Both the northern and southern axial segments recently have moved or jumped westward; perhaps the central segment will be next.

2.3. Sea-floor spreading rates

Based on Figure 9 and additional magnetic profiles from the six short survey lines (shown in Rea, 1975a), anomalies were selected representing the Gilsa event, Jaramillo event, and Brunhes/Matuyama reversal boundary with mid-point ages of 1.7, 0.92, and 0.69 m.y., respectively (Cox, 1969). Using distances between the mid-points of the anomalies and the summit of the axial block, spreading rates for the last 1.7 m.y. were determined by linear regression. Only those anomalies that appeared symmetrical about the axis were used for the regression in order to avoid any bias from the asymmetrically situated anomalies south of the small offset at 11.5°S. A t-value of 0.0 m.y. and an x-value of 0.0 ±2 km were assigned to the summit of the axial block for the regression. Results are given in Table I. Sea-floor spreading anomalies are not well developed here because of reasons given above and

TABLE I

Spreading rates in mm/y or km/m.y. for the East Pacific Rise, 9.5°S to 12°S

Interval	Rate		
	West flank	East flank	Total
Gilsa–Jaramillo	76.7 ± 2.5[a]	74.5 ± 2.2	151.2 ± 3.3
Jaramillo–Brunhes/Matuyama	91.0 ± 4.4	75.9 ± 5.2	166.9 ± 6.8
Brunhes/Matuyama–Axis	79.0 ± 1.1	81.1 ± 1.4	160.1 ± 1.8
Gilsa–Jar.–B/M –Axis	79.9 ± 1.0	77.3 ± 0.9	157.2 ± 1.3

[a] Errors are 1-standard deviation, and assumed to be independent in addition ($E_w^2 + E_e^2 = E_t^2$).

so the errors shown in Table I are probably a better indication of statistical precision than of geological accuracy.

Overall, since Gilsa time, the west flank of the EPR has been spreading slightly faster (80 mm/y) than the east flank (77 mm/y). Spreading rates for each of the anomaly pairs show small differences on each flank, but only those for the Jaramillo-Bruhnes/Matuyama time interval may be real. The rapid spreading rate of the west flank during this time interval is derived using 13 data points. If this were the result of a small axial jump, one would expect a corresponding decrease in the east flank rates, but this is not observed (Table I).

If all apparent asymmetries in sea-floor spreading rates were the result of a migrating rise axis, the total separation rates should remain the same. This, however, does not seem to be the case. The last column in Table I shows that total separation rates may have increased since the Gilsa to Jaramillo time interval, 1.7 to 0.9 m.y. ago. The existing data do not provide information as to whether this increase is a single event or part of a cyclical variation in spreading rates about some average value. Blakely (1975) has demonstrated variations in spreading rates of up to 40% of the total rate from studies of magnetic anomalies southwest of the Blanco fracture zone in the northeast Pacific. Information presented above suggests that the rate variations observed by Blakely might result from either small changes in the position of the axis or true changes in spreading rates. Both types of variation occur in the 9.5°S to 12°S region of the East Pacific Rise.

3. Eastern Flank of the East Pacific Rise

3.1. A MAGNETIC-ANOMALY ISOCHRON

The east flank of the EPR extends from the axis, along about 110°W, to the western edge of the Bauer Deep, along 104°W, an east-west distance of almost 700 km (Figures 1 and 8). Within this distance only one magnetic anomaly older than the Gilsa anomaly, anomaly 3′ (Talwani *et al.*, 1971), can be correlated with any certainty across the region. Several anomalies occurring on all lines between approximately 106.9°W and 107.8°W (Figure 9) are part of anomaly 3, but individual peaks cannot be correlated with any confidence across the region.

Anomaly 3′ can be correlated across five magnetic profiles, resulting in a trend similar to that of the rise axis (Figures 8 and 9). This anomaly is either offset about 10 km near 12.3°S, indicating another small axial offset, or changes trend near line KK-71-7 at 12°S. The peak of anomaly 3′ occurs at the boundary between the predominantly normal Epoch 5 and the younger, predominantly reversed Gilbert epoch. Unfortunately, the exact age of anomaly 3′ is subject to some debate. Ages given for the Gilbert-Epoch 5 reversal include 5.61 m.y. (Heirtzler *et al.*, 1968), 5.5 m.y. (Vine, 1968), 5.05-5.1 m.y. (Opdyke and Foster, 1970; Foster and Opdyke, 1970; Opdyke, 1972), and 5.18 m.y. (Talwani *et al.*, 1971). The first two ages are based on marine magnetic-anomaly profiles, the third and youngest age estimate is

based on magnetic reversals recorded in marine sediments and the last estimate upon a combination of the two methods.

These ages can be further modified by dating terrestrial volcanics of known magnetic polarity. Normally polarized rocks 4.8 ± 0.15, 5.03 ± 0.13, and 5.06 ± 0.15 m.y. old (Dalrymple *et al.*, 1967) seem contrary to the suggestion of a normal to reverse polarity change at 5.2 m.y. ago. Reversely polarized lava flows dated at 5.37 ± 0.07 m.y. (Watkins *et al.*, 1971), 5.3 ± 0.2 m.y. (Mankinen, 1972) and 5.35 ± 0.11 m.y. (Watkins, 1973) probably lie within the Gilbert reversed epoch and therefore are younger than the reversal at the beginning of the Gilbert. Obviously, the assumption of constant sedimentation rate and of constant sea-floor spreading rate basic to many of these estimates are open to some question. However, errors in the dating of rocks can be at least partially quantified and expressed as an error range. Thus, an age of 5.4 m.y. will be used for anomaly 3'.

The distance from the central portion of the EPR axis (that part not offset to the west during the last 1.7 m.y.) to anomaly 3' is 465 km. At the assumed age of 5.4 m.y. for this anomaly, the overall spreading rate for the east flank of the EPR in this region has been about 86 mm/y, somewhat higher than the more recent east-flank rates of about 77 mm/y for the past 1.7 m.y. (Table I). This rate is only approximate, however, as uncertainties in the east-flank spreading rate arising from possible asymmetrical spreading, shifts in the position of the axis, and uncertainty in the dating of anomaly 3' must remain.

3.2. Regional morphology

The general morphology of the east flank of the East Pacific Rise between 9.5°S and about 12°S is illustrated in Figure 10 which shows bathymetric profiles from five long east-west trending lines that traverse this part of the ocean floor. The topography on the rise flank, like that in the 10.5°S survey area, shows features a few kilometers wide superimposed on broader forms a few tens of kilometers wide (Figure 10, middle three lines). Overall relief is 100 to 200 meters except in the region of rough topography lying between 106°W and 107°W on the *Chain*-100 and Amphitrite tracklines in the northern part of the area and in a region of rough, blocky topography about 90 km wide lying along the eastern edge of crust generated by the modern EPR (Figure 10).

One consequence of the steady-state elevation model of mid-ocean (Sclater and Francheteau, 1970; Sclater *et al.*, 1971) is that portions of the sea floor generated at different spreading rates should have different slopes. Such a topographic age-depth model has been used by several workers to demonstrate changes in spreading rates (cf. Vogt *et al.*, 1969; van Andel and Heath, 1970). It is tempting, therefore, to suggest that the two regional changes in slope at about 105.5°W and 3800 m depth, and 109° to 109.5°W and 3400 m (Figures 10 and 11) might be the result of slower spreading prior to about 6.0 m.y. ago when the EPR was starting anew in cold lithosphere, then faster spreading from about 6.0 to 2.0 m.y. ago resulting in a more gentle slope, and finally slower spreading from about 2 m.y. ago until the present.

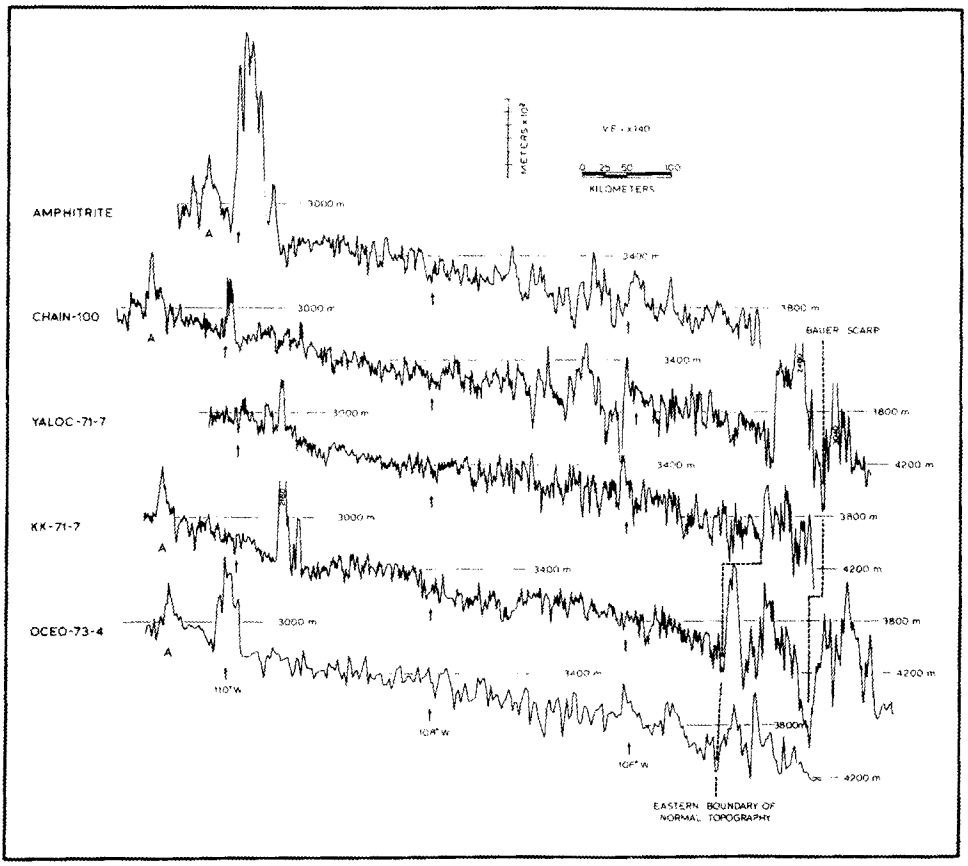

Fig. 10. Bathymetric profiles across the east flank of the EPR. Profile locations on Figure 8. A denotes EPR axis, arrows indicate where profiles cross 110°, 108°, and 106° W. Dashed lines indicate topographic correlations. Differences in fine-scale morphology are the result of varying data digitizing procedures employed by institutions supplying data.

Such a sequence would explain the slope changes (Figure 11) and is in accord with the observation that spreading between 0 and 1.7 m.y. ago seems to be slower than the overall rate back to 5.4 m.y. ago.

Parker and Oldenburg (1973) and Davis and Lister (1974) have shown that the depth (h) of the sea floor can be expressed as a function of its age (t). Davis and Lister found that the slope of the line defined by $ht^{-1/2}$ is reasonably constant in any given area. Such a curve for the east flank of the EPR can be constructed on the basis of four known data points – the sea-floor depths at points of known age (Table II). The axis is not included in the data used to define the relationship because constructional processes most likely occur there (Rea, 1975b). For the east flank of the EPR between 9° and 13°S, the relationship $h(\text{km}) = 0.40\, t(\text{m.y.})^{1/2} + 2.82$ is defined by the four data points (Figure 11, inset). The difference between the observed axial depth, 2700 m. and the calculated depth at $t = 0$, 2820 m, may be a crude estimate of the amount of extrusive activity occurring along the spreading center.

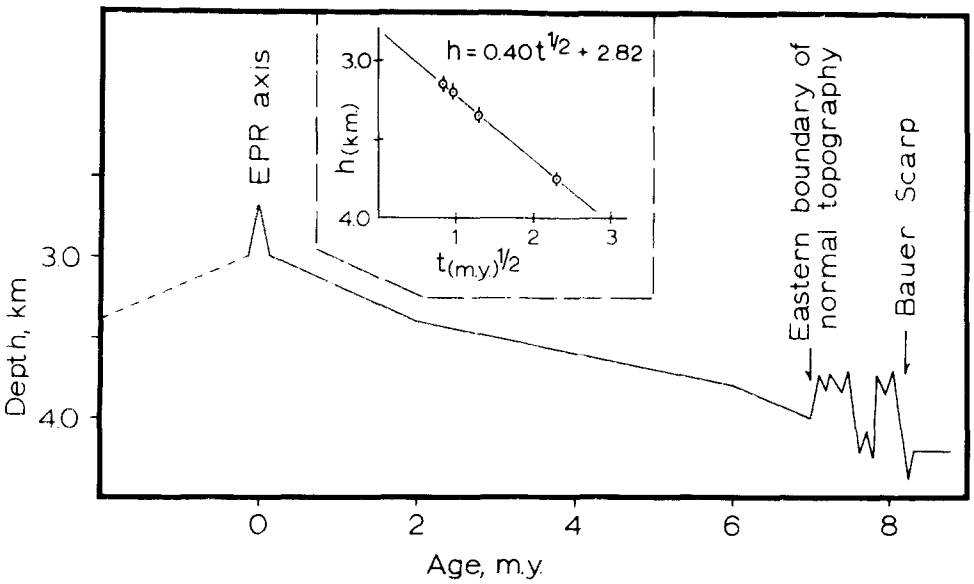

Fig. 11. Regional topographic features and slopes generalized from profiles shown on Figure 10. EPR axis, slope breaks at 2 m.y., 3400 m, and 6 m.y., 3800 m, and the region of blocky topography along the eastern edge of the modern EPR are illustrated. Inset at top shows plot depth in km (h) vs square root of age in m.y. ($t^{1/2}$).

The derived age-depth relation $h = 0.40\,t^{1/2} + 2.82$ can be used to check the age of the slope changes at about 3400 and 3800 m depth (Figures 10 and 11). These ages turn out to be 2.1 and 6.0 m.y., respectively, confirming the above estimates. Knowing the spreading rate for the time 0 to 2 m.y. ago (77 mm/y) and the overall spreading rate back to 5.4 m.y. ago (86 mm/y) we can now calculate the faster spreading rate between 2 and 5.4 m.y. ago, which was approximately 90 mm/y.

Four of the lines in Figure 8 cross the eastern edge of the modern EPR, which is also the western boundary scarp of the Bauer Deep (Figure 1), hereafter referred to as the Bauer Scarp (Figures 8 and 10). Sclater *et al.* (1971) have shown that when a new spreading system begins in old crust and starts to generate new sea floor, the topographic profile across this new feature should have gentle slopes rising to the axis on the top and steep sides which are scarps separating older and younger sea floor.

TABLE II

Sea-floor depths at points of known age, EPR east flank, 9° to 13°S

t (age, m.y.)	$t^{1/2}$	h (depth, km)
0.69	0.831	3.150 ± 0.05
0.92	0.959	3.200 ± 0.05
1.70	1.304	3.350 ± 0.05
5.40	2.324	3.750 ± 0.05

The deep hole shown on lines *Chain*-100 and KK-71-7 in Figure 10 and also observed on other crossings of this feature probably represents this scarp. The age of this scarp dates the time of inception of the modern EPR.

Herron (1972) dated the beginning of activity on the modern EPR at about 9 m.y. ago from a preliminary analysis of magnetic anomaly data. Anderson and Sclater (1972) have suggested an age of about 6.5 m.y. for the initiation of spreading along the northern EPR from an analysis of sea floor age-depth relationships, but they have only one crossing of the Bauer Scarp in the region of 9.5° to 12°S.

South of the 9°S fracture zone, which intersects the Bauer Deep and Scarp near 10°S, 104°W, the western limit of higher-relief, blocky sea-floor topography can be correlated between the Oceo-73-4, KK-71-7, and YALOC-71-7 tracklines (Figures 8 and 10). This topographic change occurs along a line roughly parallel to anomaly 3′, and may mark the place, and therefore the time, where the moden EPR had completed the process of jumping, heating and cracking the initially cold lithosphere, and begun to function normally. A similar topographic change can be seen on the lower flanks of other rises that have originated after large jumps in spreading activity during the last 8 or 10 m.y., such as the northern EPR near the Orozco fracture zone (Sclater *et al.*, 1971, their Figures 8 and 9), and the part of the EPR between the 6.5°S and 9°S fracture zone (Rea, 1975a).

Knowing the distance from anomaly 3′ to the Bauer Scarp, about 230 km, and to the location of the change in topographic character, about 140 km (Figure 8), and the approximate spreading rates for the region we can compute the time of initiation of the modern EPR and the time when it began to produce low-relief ordinary abyssal topography. The regional slope of the sea floor generated prior to 6 m.y. ago is similar to that generated during the most recent 2 m.y., implying that the spreading rates for the two periods were also similar. The older spreading rate is therefore assumed to be 80 mm/y. From this information, the time of initiation of the modern EPR is estimated to be approximately 8.2 m.y. ago, and the time when it began to function smoothly to be about 7.1 m.y. ago. Calculated sea-floor depth at 7.1 m.y. is 3885 (±50) m, slightly shallower than the observed depth of 3900 to 4000 m observed at this topographic boundary.

4. Discussion

4.1. Development of topographic features

Using the bathymetric information from the 10.5°S survey area together with previously published data, it is possible to construct an empirical model that explains the formation of both the axial block and the adjacent abyssal topography. The model, discussed more fully elsewhere (Rea, 1975b), involves extrusion of lava along the axis to form the axial block followed by down-faulting of the sides of the block as the material moves laterally off the top of the supporting magma column. Asymmetrical abyssal hills tilted outward from the axis have been found associated with the EPR at 10.5°S and with other Pacific spreading centers (Larson, 1971; Krause *et al.*,

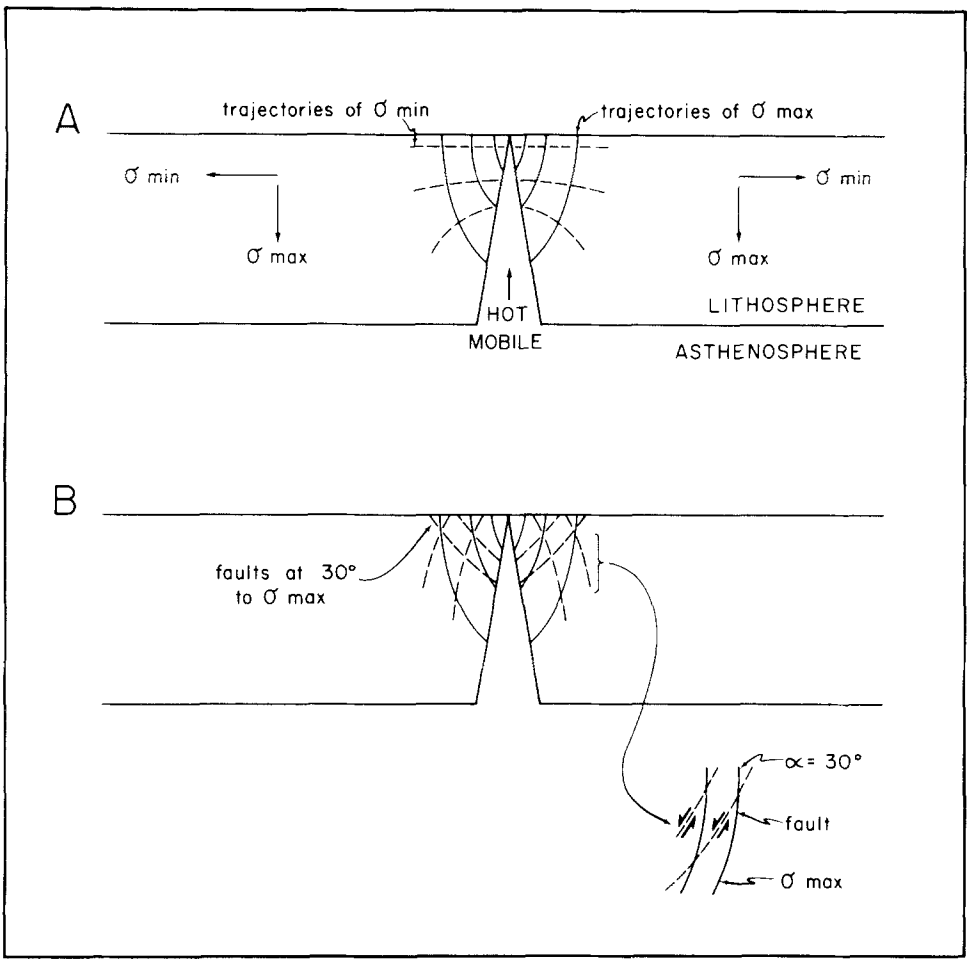

Fig. 12. Orientation of stresses and resulting fault orientation within the brittle layer of the lithosphere at a fast-spreading rise crest. Stress trajectories shown in A, with the intermediate stress axis perpendicular to the plane of the figure. Resulting fault patterns shown in B. Modified from Hafner (1951).

1973; Klitgord and Mudie, 1974), implying that the origin of the hills is not related to local axial topography, which is variable, but rather to a more fundamental phenomenon.

Stresses associated with the spreading center (Figure 12) are oriented such that the tensional or minimum compressive stress axis is horizontal at the ocean floor and perpendicular to the rise crest. The maximum stress is lithostatic and vertical at the ocean-floor surface. At a given depth below the top of the basalt, lithostatic stress will be greater on the flanks of the rise than over the crest because of higher density of overburden, resulting in a relative upward force under the accreting plate edges. Stress trajectories and the resulting faulting expected in a horizontal slab subjected to lateral tension and a relative upward force in the middle have been calculated by Hafner (1951). Under these conditions, the trajectories of maximum stress will be

vertical at the surface but bent toward the point of relative upward force in the middle (Hafner, 1951; Figure 12A). Faults resulting from this stress field will dip towards the axis at about 60° at the surface but will decrease in dip with depth (Figure 12 B). Downfaulting along these curved fault surfaces will rotate the tops of the fault blocks outward away from the axis to produce the tilted abyssal hills observed (Rea, 1975b).

4.2. Axis shifts and asymmetrical spreading

The most interesting aspect of the spreading regime at 10°S is the occurrence of abrupt changes in the position of the spreading center. The two axial dislocations at 10.0° and 11.5°S are well documented, of small magnitude and have left no traces in the bathymetry. It is possible that other small axial shifts have occurred that are not recorded in either the bathymetry or the rather poorly defined magnetic anomalies occurring on this portion of the EPR. That two dislocations have occurred since 1.7 m.y. ago, where there are enough data to define them, suggests that such a process may not be unusual for fast-spreading rises.

Along the section of the EPR shown in Figure 8, axis shifts of both the northern and southern segments have been in the same direction, to the west. This process, whether caused by small axis jumps or local episodes of highly asymmetric spreading, simulates regional asymmetrical spreading and may explain this phenomenon on other fast-spreading rises. Small jumps of a symmetrically spreading axis would not seriously disturb the magnetic-anomaly isochrons, would leave no topographic trace, and could not easily be distinguished from asymmetrical spreading from a stationary axis. Asymmetrical spreading has been observed on the EPR south of the Easter Island triple-point and north of the Eltanin fracture zone at 56°S (Herron, 1971) where the distance between the rise axis and anomaly 5 is greater on the east flank than to the west. Herron (1971) has suggested westward axial migration as one probable cause of this situation. This westward migration may have been accomplished by a series of either small westward axial jumps or local episodes of symmetric spreading.

Asymmetric spreading observed on the Southeast Indian Ridge south of Australia where the total rate of crustal generation is about 70 mm/y appears to be continuous on the scale of 10 km (Hayes, 1976) in contrast to the discrete axis shifts of that same magnitude observed on the EPR at 10.0° and 11.5°S.

4.3. A remaining question

Perhaps the most interesting problem raised by this study concerns the mechanism by which the small axis shifts occur. Two methods, discussed above, appear possible, neither of which leave any bathymetric trace. The first entails faults bounding the axial block tapping the underlying magma chamber, followed by downfaulting of the prior axial block, possibly in sections, to become abyssal hills. The second method involves an episode of true asymmetrical accretion confined to a specific segment of the rise axis in both space and time. If the first alternative were the correct one, we

might expect to see a double axial block should this process be observed when only partially completed. The second process has occurred on a large scale south of Australia (Hayes, 1976) but it is more difficult to imagine on a smaller scale, 150 km length of axis and restricted to one or two million years.

To determine which of these processes is more likely, it will be necessary to survey a portion of rise crest in the process of shifting and the gradiational zone to the adjacent stationary axis segment. Additionally, the survey should be located in a region where the sea-floor spreading magnetic anomalies are better developed than they are in the 10.5°S survey area, so that the extent of possible spreading asymmetries may be determined more accurately.

4.4. Summary of Geologic History

The geologic history of the East Pacific Rise between the 9°S fracture zone and about 12°S began in late Miocene time when the locus of sea-floor spreading activity in the southeastern Pacific jumped westward from the now fossilized Galapagos Rise (Figure 1) to a position about 900 km down its flank (Herron, 1972). The new spreading center must have begun by heating, expanding, and finally cracking the initially cold lithosphere. With the completion of the initial heating and expansion, the new axis of activity began to generate oceanic crust slightly over 8 million years ago. By 7 m.y. ago, the new spreading center was functioning normally. About 6 m.y. ago the spreading rate increased from approximately 80 mm/y to 90 mm/y and then approximately 2 million years ago, decreased to 80 mm/y or less. Some time between 1.7 and 0.9 m.y. ago the northern third of the EPR axis shifted westward a distance of less than 10 km. Also during this interval, the southern part of the EPR axis within the 10.5°S survey area changed trend. Since the Brunhes/Matuyama reversal at 0.69 m.y. ago, the southern part of the axis, south of 11.5°S, shifted westward a distance of 7 or 8 km. At present, sea-floor spreading is continuing along this portion of the EPR at a total rate of 160 mm/y.

Acknowledgements

As in any regional study, data for this report were provided by many sources. Data from the *Conrad*-11 cruise of the Lamont-Doherty Geological Observatory were provided by the following people: magnetic data, W. C. Pitman III; bathymetry, D. E. Hayes, Submarine Morphology Department. R. P. von Herzen of Woods Hole Oceanographic Institute provided data from the *Chain*-100 cruise. Data from the Amphitrite cruise of the Scripps Institution of Oceanography were forwarded by T. Chase.

G. R. Heath of Oregon State University and D. M. Hussong of the Hawaii Institute of Geophysics, were chief scientists aboard the *Yaquina* and *Kana Keoki*, respectively, during the completion of the 10.5°S rise crest survey. L. W. Kroenke of HIG completed the initial reduction of data from the *Kana Keoki* cruises and B. H.

Erickson, N.O.A.A. Pacific Marine Environmental Laboratory provided data from the *Oceanographer* cruises.

L. D. Kulm and Tj. H. van Andel provided encouragement and advice throughout this study which forms a portion of a Ph.D. thesis submitted to Oregon State University. K. Keeling, S. Derks, and N. G. Pisias assisted with the data processing and computer programming.

L. D. Kulm and G. R. Heath reviewed this paper and provided many helpful comments and suggestions.

This study was supported by the National Science Foundation via the IDOE Nazca Plate Project Grant No. GX-28675.

References

Anderson, R. N. and Noltimier, H. C.: 1973, 'A Model for the Horst and Graben Structure of Mid-ocean Ridge Crests Based upon Spreading Velocity and Basalt Delivery to the Oceanic Crust', *Roy. Astron. Soc. Geophys. J.* **34**, 137–147.

Anderson, R. N. and Sclater, J. G.: 1972, 'Topography and Evolution of the East Pacific Rise Between 5° and 20°S', *Earth and Planetary Sci. Letters* **14**, 433–441.

Atwater, T. and Mudie, J. D.: 1973, 'Detailed Near-Bottom Geophysical Study of the Gorda Rise', *J. Geophys. Res.* **78**, 8665–8686.

Blakely, R. J.: 1975, 'Evidence of Local Migration of a Spreading Center', *Geology* **3**, 35–38.

Cox, A.: 1969, 'Geomagnetic Reversals', *Science* **163**, 237–245.

Dalrymple, G. B., Cox, A., Doell, R. R., and Gromme, C. S.: 1967, 'Pliocene Geomagnetic Polarity Epochs', *Earths and Planetary Sci. Letters* **2**, 163–173.

Davis, E. E. and Lister, C. R. B.: 1974, 'Fundamentals of Ridge Crest Topography', *Earth and Planetary Sci. Letters* **21**, 405–413.

Dobrin, M. B.: 1960, *Introduction to Geophysical Prospecting*, McGraw-Hill, New York, N.Y., 446 p.

Foster, J. H. and Opdyke, N. D.: 1970, 'Upper Miocene to Recent Magnetic Stratigraphy in Deep-sea Sediments', *J. Geophys. Res.* **75**, 4465–4473.

Hafner, W.: 1951, 'Stress Distributions and Faulting', *Geol. Soc. Am. Bull.* **62**, 373–398.

Hayes, D. E.: 1976, 'The Nature and Implications of Asymmetric Sea-floor Spreading', *Geol. Soc. Am. Bull.*, in press.

Heirtzler, J. R., Dickson, G. O., Herron, E. M., Pitman, W. C., III, and Le Pichon, X.: 1968, 'Marine Magnetic Anomalies, Geomagnetic Field Reversals and Motions of the Ocean Floor and Continents', *J. Geophys. Res.* **73**, 2119–2136.

Herron, E. M.: 1971, 'Crustal Plates and Sea Floor Spreading in the Southeastern Pacific', *Am. Geophys. Union, Antarctic Oceanology I, Antarctic Research Series* **15**, 229–237.

Herron, E. M.: 1972, 'Sea-floor Spreading and the Cenozoic History of the East-Central Pacific', *Geol. Soc. Am. Bull.* **83**, 1671–1692.

I.A.G.A. Commission 2 Working Group 4, Analysis of the Geomagnetic Field: 1969, 'International Geomagnetic Reference Field 1965.0', *J. Geophys. Res.* **74**, 4407–4408.

Klitgord, K. D. and Mudie, J. D.: 1974, 'The Galapagos Spreading Centre: a Near-Bottom Geophysical Survey', *Roy. Astron. Soc. Geophys. J.* **38**, 563–586.

Krause, D. C., Grim, P. J., and Menard, H. W.: 1973, *Quantitative Marine Geomorphology of the East Pacific Rise*, Nat'l. Oceanic and Atmospheric Admin. Tech. Rept. ERL 275-AOML 10, 73 pp.

Larson, R. L.: 1971, 'Near-bottom Geologic Studies of the East Pacific Rise Crest', *Geol. Soc. Am. Bull*, **82**, 823–841.

Luyendyk, B. P.: 1970, 'Origin and History of Abyssal Hills in the Northeast Pacific Ocean', *Geol. Soc. Am. Bull.* **81**, 2237–2260.

Mammerickx, J., Anderson, R. N., Menard, H. W., and Smith, S. M.: 1975, 'Morphology and Tectonic Evolution of the East-central Pacific', *Geol. Soc. Am. Bull.* **86**, 111–118.

Mankinen, E. A.: 1972, 'Paleomagnetism and Potassium-Argon Ages of the Sonoma Volcanics, California', *Geol. Soc. Am. Bull.* **83**, 2063–2072.

Matthews, D. J.: 1939, *Tables of the Velocity of Sound in Pure Water and Sea Water for Use in Echo-sounding and Sound-ranging* (2nd ed.), Hydrographic Dept. Admiralty, London, 52 pp.

Opdyke, N. D.: 1972, 'Paleomagnetism of Deep-Sea Cores', *Rev. Geophys. Space Phys.* **10**, 213–249.

Opdyke, N. D. and Foster, J. H.: 1970, 'Paleomagnetism of Cores from the North Pacific', in Hays, J. D. (ed.), *Geological Investigations of the North Pacific*, Geol. Soc. America Mem. 126, Boulder, Co., pp. 83–119.

Parker, R. L. and Oldenburg, D. W.: 1973, 'Thermal Model of Ocean Ridges', *Nature Phys. Sci.* **242**, 137–139.

Rea, D. K.: 1972, 'Magnetic Anomalies along Fracture Zones', *Nature Phys. Sci.* **236**, 58–59.

Rea, D. K.: 1975a, *Tectonics of the East Pacific Rise, 5° to 12°S*', (Ph.D. Thesis), Corvallis, Oregon State University, 139 pp.

Rea, D. K.: 1975b, 'Model for the Formation of Topographic Features of the East Pacific Rise Crest', *Geology* **3**, 77–80.

Rea, D. K., and Naugler, F. P.: 1971, 'Musicians Seamount Province and Related Crustal Structures North of the Hawaiian Ridge', *Marine Geol.* **10**, 89–111.

Rea, D. K., Dymond, J., Health, G. R., Heinrichs, D. F., Johnson, S. H., and Hussong, D. M.: 1973, 'New Estimates of Rapid Seafloor Spreading Rates and the Identification of Young Magnetic Anomalies on the East Pacific Rise, 6° and 11°S', *Earth and Planetary Sci. Letters* **19**, 225–229.

Scheidegger, K. F.: 1973, 'Temperatures and Compositions of Magmas Ascending Along Mid-ocean Ridges', *J. Geophys. Res.* **78**, 3340–3355.

Schouten, J. A.: 1971, 'A Fundamental Analysis of Magnetic Anomalies over Oceanic Ridges', *Marine Geophys Res.* **1**, 111–144.

Sclater, J. G. and Francheteau, J.: 1970, 'The Implications of Terrestrial Heat Flow Observations on Current Tectonic and Geochemical Models of the Crust and Upper Mantle of the Earth', *Roy. Astron. Soc. Geophys. J.* **20**, 509–542.

Sclater, J. G., Anderson, R. N., and Bell, M. L.: 1971, 'Elevation of Ridges and the Evolution of the Central Eastern Pacific', *J. Geophys. Res.* **76**, 7888–7915.

Talwani, M., Windisch, C. C., and Langseth, M. G., Jr.: 1971, 'Reykjanes Ridge Crest: a Detailed Geophysical Study', *J. Geophys. Res.* **76**, 473–517.

van Andel, Tj. H., and Heath, G. R.: 1970, 'Tectonics of the Mid-Atlantic Ridge 6–8° South Latitude', *Marine Geophys. Res.* **1**, 5–36.

Vine, F. J.: 1968, 'Magnetic Anomalies Associated with Mid-ocean Ridges', in Phinney, R. A. (ed.), *The History of the Earth's Crust*, Princeton Univ. Press, Princeton, N.J., pp. 73–89.

Vogt, P. R., Avery, O. E., Schneider, E. D., Anderson, C. N., and Bracey, D. R.: 1969, 'Discontinuities in Sea-floor Spreading', *Tectonophys.* **8**, 285–317.

Watkins, N. D.: 1973, 'Paleomagnetism of the Canary Islands and Madeira', *Roy. Astron. Soc. Geophys. J.* **32**, 249–267.

Watkins, N. D., Gunn, B. M., Baksi, A. K., York, D., and Ade-Hall, J.: 1971, 'Paleomagnetism, Geochemistry, and Potassium–Argon Ages of the Rio Grande de Santiago Volcanics, Central Mexico', *Geol. Soc. Am. Bull.* **82**, 1955–1968.